

Vibrational spectrum renormalization by enforced coupling across the van der Waals gap between MoS₂ and WS₂ monolayers

Wen Fan,¹ Xi Zhu,² Feng Ke,³ Yabin Chen,¹ Kaichen Dong,¹ Jie Ji,⁴ Bin Chen,³ Sefaattin Tongay,⁵ Joel W. Ager,⁶ Kai Liu,⁷ Haibin Su,^{2,*} and Junqiao Wu^{1,6,†}

¹*Department of Materials Science and Engineering, University of California, Berkeley, California 94720, USA*

²*School of Materials Science and Engineering, Nanyang Technological University, Singapore 639798, Singapore*

³*Center for High Pressure Science and Technology Advanced Research, Shanghai 201203, China*

⁴*Department of Thermal Science and Energy Engineering, University of Science and Technology of China, Hefei, Anhui 230027, China*

⁵*School of Engineering of Matter, Transport and Energy, Arizona State University, Tempe, Arizona 85287, USA*

⁶*Materials Sciences Division, Lawrence Berkeley National Laboratory, Berkeley, California 94720, USA*

⁷*School of Materials Science and Engineering, Tsinghua University, Beijing 100084, China*

(Received 22 July 2015; revised manuscript received 26 October 2015; published 18 December 2015)

At the few or monolayer limit, layered materials define an interesting two-dimensional system with unique electronic and phonon properties. The electron band structure of monolayers can be drastically different from multilayers despite the weak van der Waals interaction between neighboring layers. In this Rapid Communication, we demonstrate that vibrational spectra of a MoS₂ monolayer and a WS₂ monolayer are also renormalized when the interaction between them is artificially modulated. This is achieved by using a diamond-anvil cell to apply high pressures, up to 39 GPa onto WS₂/MoS₂ heterobilayers. With increasing pressure, the out-of-plane Raman frequencies of the two individual monolayers repel each other, exhibiting coherent vibrations across the van der Waals gap with an optical-like and an acousticlike interlayer vibration mode. The discovery shows a crossover in lattice vibration from a two-dimensional system toward a three-dimensional system driven by enforced interlayer coupling.

DOI: [10.1103/PhysRevB.92.241408](https://doi.org/10.1103/PhysRevB.92.241408)

PACS number(s): 73.20.-r, 63.22.Np, 68.35.Ja, 68.90.+g

In layered materials, strong intralayer covalent bonds and weak interlayer van der Waals (vdW) interactions allow for separation of single-crystalline layers via mechanical or chemical exfoliation [1,2]. Although neighboring layers are held together by weak vdW interactions, physical properties of these layered semiconductors are sensitive to interlayer coupling across the vdW gap. For example, with a few exceptions (e.g., ReS₂ [3]), many semiconducting transition-metal dichalcogenides (e.g., MoS₂, WS₂, and MoSe₂) switch from indirect band gaps in the bulk or multilayers to direct band gaps in the monolayer limit [4–7]. A few other layered semiconductors (e.g., InSe) exhibit the opposite trend, i.e., switching from direct band gaps in the bulk to indirect band gaps toward the monolayer limit [8,9]. The normalization of band structure by the interlayer coupling signifies a crossover from a two-dimensional (2D) electronic system in the monolayer to a three-dimensional (3D) electronic system in the bulk. Therefore, the degree of two dimensionality, or, the “2Dness,” of the system is defined by the strength of interlayer coupling. If the interlayer coupling can be artificially reduced or enhanced, one can effectively modulate the electronic dimensionality of the system, which would offer much insight into low-dimensional physics. Indeed, this has been experimentally achieved with chemical intercalation or application of hydrostatic pressure. For instance, with the application of high hydrostatic pressures at 10–20 GPa, an

insulator-metal phase transition with a rapid drop in resistivity has been observed in bulk MoS₂ [10–12].

These studies all focus on normalization of the electronic structure with artificially tuned interlayer coupling. It is less clear how the vibrational motions of the system responds to modulation of the interlayer coupling. In bulk or multilayer materials, their Raman-active modes are found to stiffen with increasing pressure applied [10–12]. However, as the materials studied are composed of a stack of identical layers (hence homomultilayers), it is challenging to distinguish the vibrational modes from individual monolayers. In this Rapid Communication, we apply high pressure to heterobilayers composed of a MoS₂ monolayer stacked on a WS₂ monolayer and demonstrate that a dimensional crossover, similar to that observed in electronic band-structure renormalization, occurs also in the lattice vibrational structure of the system.

We measured the Raman modes of the WS₂/MoS₂ heterobilayers as well as separate MoS₂ and WS₂ monolayers under hydrostatic pressure applied using a diamond-anvil cell (DAC). The MoS₂ and WS₂ monolayers were grown by a well-established chemical vapor deposition (CVD) technique onto SiO₂/Si substrates [13,14]. The WS₂/MoS₂ heterobilayers were prepared using a polydimethylsiloxane (PDMS) stamping technique as described in previous reports [14]. Briefly, PDMS was spin coated on a CVD-grown monolayer WS₂/SiO₂/Si and cured at 120 °C for >3 h. The PDMS/WS₂ was released from the SiO₂/Si substrate by mildly etching SiO₂ in a 2 mol/L KOH solution for 0.5–2 h. It was then rinsed in de-ionized water to remove the KOH residue and transferred onto a CVD-grown monolayer MoS₂/SiO₂/Si substrate as shown in the inset of Fig. 1(a). Afterwards, the PDMS/WS₂/MoS₂ was released from the SiO₂/Si substrate by mild KOH etching again. It was then stamped onto the

*Author to whom correspondence should be addressed; hbsu@ntu.edu.sg

†Author to whom correspondence should be addressed; wuj@berkeley.edu

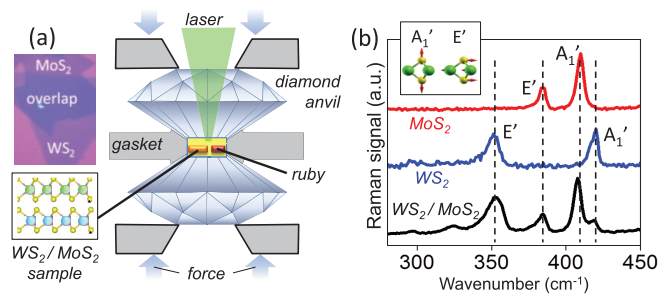


FIG. 1. (Color online) (a) Schematic of the high-pressure experiment on WS_2/MoS_2 heterobilayers using a diamond-anvil cell. The inset shows an optical image of an overlapped region between MoS_2 and WS_2 monolayers on a SiO_2/Si surface (scar bar $10\ \mu\text{m}$). (b) Raman spectra of a MoS_2 monolayer, a WS_2 monolayer, and a WS_2/MoS_2 bilayer recorded at ambient pressure ($P \approx 0$). The A_1' (out-of-plane) and E' (in-plane) peaks of each layer are labeled, and their oscillation modes are shown in the inset.

center of the diamond culet table of the DAC, and then the PDMS substrate was peeled off slowly, leaving the WS_2/MoS_2 heterobilayer on top of the diamond culet table. The sample was aligned to a small hole (diameter of $\sim 100\ \mu\text{m}$) drilled in a rhenium gasket and sealed by the two diamonds. The culet size of the diamonds is $\sim 300\ \mu\text{m}$, and the gasket was preindented to a depth of $\sim 40\ \mu\text{m}$ to ensure good alignment and tight sealing. Hydrostatic pressure near the sample was determined by the standard ruby fluorescence method. The pressure medium used in our experiments was a mixture of methanol and ethanol (4:1). The culet table was cleaned and wetted with the pressure medium prior to the sample stamping to ensure existence of the medium between the sample and the culet surface. We note that the medium may freeze at pressures higher than $\sim 10\ \text{GPa}$, which may result in slight inhomogeneities in pressure in the DAC. Raman spectroscopy was performed with a Renishaw microphotoluminescence/Raman system using an excitation laser of wavelength $532\ \text{nm}$. The Raman spectra were recorded through the DAC with a laser spot size of $\sim 2\ \mu\text{m}$ in diameter and an effective resolution of $\sim 1\ \text{cm}^{-1}$. Over 20 samples were prepared and measured, all showing consistent results with no difference seen between the two cases where MoS_2 is on top of WS_2 and the other way around or between the pressure-loading and the unloading processes.

For MoS_2 and WS_2 monolayers with the D_{3h} symmetry, there are two prominent Raman-active modes, the in-plane E' mode and the out-of-plane A_1' mode [15]. For naturally stacked homobilayers with D_{6h} symmetry, these two modes become the well-known E_{2g} and A_{1g} modes. For the WS_2/MoS_2 heterobilayers, these modes are also represented here as E' and A_1' due to the same D_{3h} symmetry as in the monolayers. There are five different stacking patterns AA1, AA3, AB1, AB2, and AB3 for such a bilayer, just like in the case of homobilayers [16]. For homomultilayers, when the number of layers increases from the monolayer, the out-of-plane A_1' mode exhibits stiffening whereas the E' mode shows softening. The former is due to enhancement in the restoration force by interactions between the S atoms from neighboring layers; the latter is attributed to enhanced dielectric screening of long-range Coulomb interaction between the metal atoms (Mo or W) because different from the vibration involving only S

atoms in the A_1' mode, in the E' mode the metal atoms also vibrate [17,18].

Typical Raman spectra of the MoS_2 monolayer, WS_2 monolayer, and WS_2/MoS_2 heterobilayers at ambient pressure ($P \approx 0$) are shown in Fig. 1(b). The out-of-plane (A_1') and in-plane (E') Raman modes of MoS_2 and WS_2 are well resolved from their monolayers [16]. All four peaks are present in the WS_2/MoS_2 heterobilayers and occur at positions identical to those of separate monolayers, indicating that the overlapped region is merely a mechanical stack of WS_2/MoS_2 bilayers without interlayer coupling. This is consistent with earlier reports that show negligible interaction between neighboring layers in as-stamped bilayers [15–18].

Upon the application of high pressure, all four Raman peaks start to shift toward higher wave numbers, accompanied with peak height reduction and width broadening. Some of the Raman spectra are selectively shown in Fig. 2(a), which compares heterobilayers and separate monolayers. The positions of these Raman peaks were determined by fitting the Raman spectra to a Lorentzian line shape and plotted in Fig. 2(b). We note that the data in Fig. 2(b) include results recorded from multiple samples as well as pressure loading/unloading. Two conclusions can be drawn from Fig. 2(b): (I) The in-plane modes (E') vary with pressure linearly, whereas the out-of-plane modes (A_1') show a nonlinear pressure dependence; (II) more interestingly, the E' modes of the heterobilayers exactly follow those of the separate monolayers, whereas the A_1' modes of the heterobilayers deviate significantly from those of separate monolayers, showing a clear repelling behavior, i.e., the stiffer A_1' mode [$A_1'(\text{WS}_2)_{\text{hetero}}$] is pushed up, whereas the softer A_1' mode [$A_1'(\text{MoS}_2)_{\text{hetero}}$] is pushed down. The fact that the E' modes of the heterobilayers precisely follow those of the separate monolayers also provides independent validation of the measurements, ruling out the possibility that the exotic pressure behavior of the A_1' modes was caused by pressure miscalibration or sample degradation. The broadening of the peaks at high pressures may be partly caused by the inhomogeneities of pressure arising from solidification of the pressure medium. The weak broad peak between 450 and $500\ \text{cm}^{-1}$ is possibly attributed to second-order Raman modes.

To understand the pressure dependence of the Raman frequencies, we have carried out a first-principles calculation of the system. All calculations were performed by density functional theory using the DMOL3 package [19,20]. All electrons are included in the simulation, and the Perdew-Burke-Ernzerhof (PBE) exchange-correlation functional with dispersion correction (PBE-D) was used [21,22]. All ions and cell parameters were fully relaxed until the force tolerance reached $0.01\ \text{eV}/\text{\AA}$ with the applied external pressure. The double numerical plus polarization basis was used for convergence tests, and a centered Brillouin zone sampled at $24 \times 24 \times 5$ was used for integration.

For calculation of the WS_2/MoS_2 heterobilayers, we sampled the five stacking patterns including AA1, AB1, AB3, AA3, and AB3 [16]. The stacking energy trend is similar to homobilayer MoS_2 [16], i.e., the AB1 and AA1 stackings are more energetically favorable than the others, and for structures (AB3 and AA3) with higher energy, the interlayer distance is larger. The stacking-dependent interlayer distance

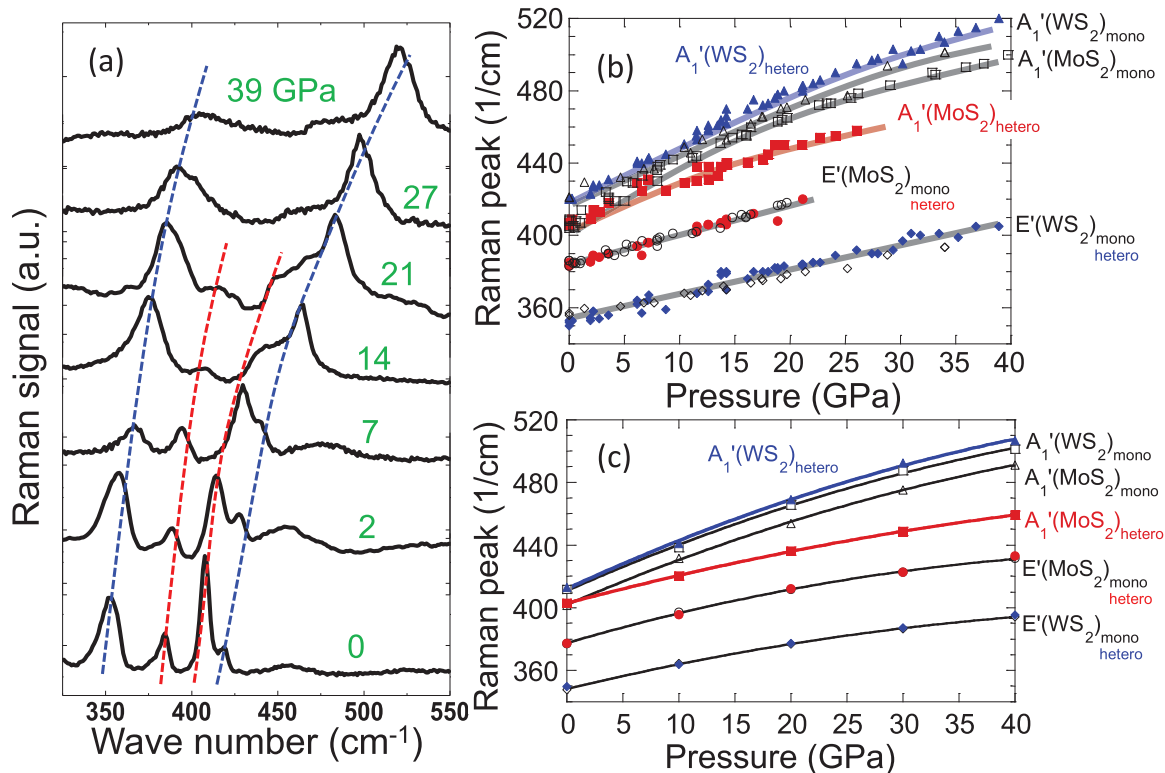


FIG. 2. (Color online) (a) Selected experimental Raman spectra recorded from a WS_2/MoS_2 heterobilayer at different pressures. The dashed lines are guides to the eye. (b) Raman peak positions of the A_1' and E' vibration modes as a function of pressure, color-coded by red (MoS_2 in the heterobilayer), blue (WS_2 in the heterobilayer), and black (both in the monolayers). The lines are guides to the eye. It can be seen that the E' modes remain the same in the bilayers as in the monolayers, whereas the A_1' modes of MoS_2 and WS_2 in the bilayer are pushed away from each other. (c) Calculated pressure-dependent A_1' and E' modes in the WS_2/MoS_2 bilayers averaged over five different stacking configurations. The calculated A_1' and E' modes of monolayer MoS_2 and WS_2 are also included as a comparison.

in WS_2/MoS_2 heterobilayers originates from the steric effect that a certain amount of space is needed between any two atoms to afford the energy cost of overlapping electron clouds, which is the same as that in the homobilayer MoS_2 [16].

As the heterobilayers are randomly stacked in our experiments, we compare the experimental results with the calculated results averaged by the five stacking patterns. Figure 2(c) shows the calculated pressure-dependent A_1' and E' frequencies averaged by the five stacking patterns of the WS_2/MoS_2 heterobilayers compared to those of the MoS_2 and WS_2 monolayers. First, we can see that the A_1' mode, which involves vibration of the S atoms only, is higher in WS_2 than in MoS_2 . The Bader charge analysis reveals that the S atom is $-0.58e$ charged in WS_2 and $-0.52e$ in MoS_2 , and therefore the Coulomb interaction is slightly stronger in WS_2 , resulting in a higher A_1' mode frequency. This is also consistent with the higher cohesive energy of WS_2 (5.78 eV) than that of MoS_2 (5.18 eV) [23].

Our calculation of the A_1' modes of the WS_2/MoS_2 heterobilayers show that these modes vibrate separately when their distance is sufficiently long. However, when an external pressure is applied, the interlayer coupling is enhanced such that the A_1' modes of the two layers turn into two coherent vibration modes where S atoms in both the MoS_2 and the WS_2 layers move in concert, one vibrating in phase and the other vibrating 180° out of phase, respectively. The two S atoms from the two layers move along the opposite (same) direction

in the coherent in-phase (out-of-phase) modes, leading to stiffened (softened) mode frequency compared to the original A_1' mode. In contrast, the in-plane E' modes in each layer are still uncoupled, even at high pressures, owing to their weak interlayer coupling.

We also found theoretically that the stacking pattern slightly affects the frequencies: For the AA3 and AB3 stackings [16], the interlayer S-S atoms are head to head to each other, which makes the A_1' mode slightly stiffer, about 3 to 4 cm^{-1} higher than the other stacking patterns. Since the E' modes are always decoupled between the two layers, there is no distinguishable difference for the E' modes between the various stacking patterns as well as with the case of the monolayers.

The pressure-induced mode stiffening can be understood from the Grüneisen parameter. The i th mode's Grüneisen parameter γ_i is computed by

$$\gamma_i = -\frac{V}{\omega_i} \frac{\partial \omega_i}{\partial V}, \quad (1)$$

where V is the volume of the unit cell. The calculated γ values are $\gamma_{A_1'}^{MoS_2} = 1.2$, $\gamma_{E'}^{MoS_2} = 1.8$, $\gamma_{A_1'}^{WS_2} = 0.6$, and $\gamma_{E'}^{WS_2} = 0.5$, in good agreement with previous results [24]. Since γ_i is positive, the frequency ω_i will increase with reduced V caused by external pressure P as observed in Figs. 2(a) and 2(b).

To better understand the vibrational spectrum normalization, we model the process with a weakly coupled

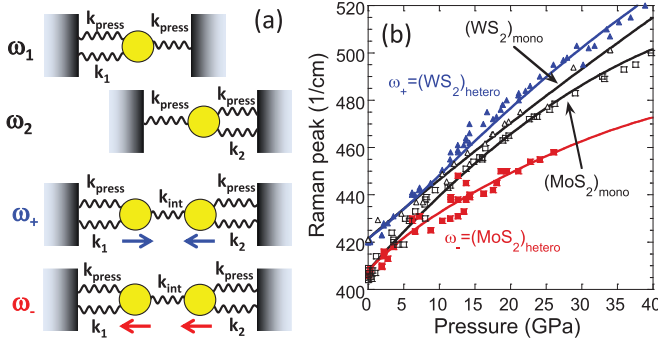


FIG. 3. (Color online) (a) Schematic of the model of two coupled harmonic oscillators, leading to two renormalized vibration frequencies (ω_{\pm}) by enforced coupling (k_{int}). The arrows indicate the vibration directions for the coupled cases, representing the optical-like and acousticlike modes for the coupled system. (b) Fitting to the measured A'_1 frequencies in heterobilayers [(WS_2)_{hetero}, blue, and (MoS_2)_{hetero}, red] using the model in (a). The lines through the monolayer A'_1 frequencies [(WS_2)_{mono} and (MoS_2)_{mono}, black] are guides to the eye.

harmonic-oscillator system. As the lattice of the bilayer system is much stiffer in the plane than out of the plane, the deformation effect from the hydrostatic pressure on the system can be considered as a uniaxial pressure applied in the out-of-plane direction. As shown in Fig. 3(a), the out-of-plane mode of the two separate monolayers (one for MoS_2 and the other for WS_2) is modeled by two separate harmonic oscillators vibrating at their eigenfrequencies,

$$\omega_{1,2} = \sqrt{(k_{1,2} + 2k_{\text{press}})/m}, \quad (2)$$

where $k_{1,2}$ is the intrinsic spring constant when the monolayers are free-standing and k_{press} is the added stiffness of the spring constant by interactions of the monolayer at its two sides with the pressure medium, which is expected to increase with pressure. We note that as the A'_1 mode involves vibration of the sulfur atoms only [Fig. 1(b) inset], the difference in the mass of cations (Mo and W) does not play a role in the discussion, and the effective mass m in Eq. (2) is set the same for ω_1 and ω_2 . When a coupling with spring constant k_{int} is introduced between the two oscillators, the new eigenfrequencies (ω_{\pm}) of the system are given by solving the coupled equation of motion,

$$\omega_{\pm}^2 = \frac{1}{2}(\omega_1^2 + \omega_2^2) + \omega_{\text{int}}^2 - \omega_{\text{press}}^2 \pm \frac{1}{2}\sqrt{(\omega_1^2 - \omega_2^2)^2 + 4\omega_{\text{int}}^4}, \quad (3)$$

where $\omega_{\text{int}} = \sqrt{k_{\text{int}}/m}$ and $\omega_{\text{press}} = \sqrt{k_{\text{press}}/m}$. It can be seen that ω_+ and ω_- correspond to oscillation modes in which the two masses are vibrating in phase and 180° out of phase, akin to the conventional optical and acoustic phonon modes in a crystal, respectively. As a result, they are stiffened and softened, respectively, from the original frequencies (ω_1 and ω_2): $\omega_+ > \omega_1 > \omega_2 > \omega_-$. However, due to the difference between ω_{int} and ω_{press} , the amounts of stiffening and softening are not equal to each other: $|\omega_+ - \omega_1| \neq |\omega_2 - \omega_-|$, which is evident from the experimental data in Fig. 2(b). This is different from a conventional hybridization problem (i.e., when $\omega_{\text{int}} = \omega_{\text{press}}$) in which the splitting in energy is expected to be symmetric. The fact that $|\omega_+ - \omega_1| < |\omega_2 - \omega_-|$ as

seen in Fig. 2(b) suggests $\omega_{\text{int}} < \omega_{\text{press}}$ or $k_{\text{int}} < k_{\text{press}}$, i.e., the interaction between the MoS_2 and the WS_2 layers is weaker than that between the monolayer and the pressure medium.

In order to apply quantitatively this analytical model to our data, we assume, to the first-order approximation, that both k_{int} and k_{press} rise linearly with pressure such that $k_{\text{int}}/m = \beta_{\text{int}}P$ and $k_{\text{press}}/m = \beta_{\text{press}}P$, where β_{int} and β_{press} are two constants related to the Grüneisen parameter of these two interactions. Equation (3) is used to fit simultaneously to the pressure dependence of the two A'_1 modes of WS_2/MoS_2 heterobilayers as shown in Fig. 3(b). In the fitting, the experimentally measured pressure dependencies of ω_1 and ω_2 of separate monolayers are directly used as the input, and β_{int} and β_{press} are adjusted as the only fitting parameters. A least-squares fitting to ω_+ and ω_- is shown in Fig. 3(b), which yields $\beta_{\text{int}} = 625 \pm 50/\text{cm}^2 \text{ GPa}$ and $\beta_{\text{press}} = 825 \pm 50/\text{cm}^2 \text{ GPa}$. The strength of these interactions can be gauged by comparing to the intrinsic A'_1 frequencies: At the maximum pressure ($P \sim 40 \text{ GPa}$) attained in this Rapid Communication, the interlayer coupling k_{int} results in a significant shift in A'_1 frequency by $158/\text{cm}$, or $\sim 39\%$. This large change is not surprising considering that the out-of-plane Young's modulus is estimated to be only $\sim 7 \text{ GPa}$ for these van der Waals crystals [25]. Therefore, high pressure through the DAC is indeed a very effective means to modulate the interlayer coupling across the van der Waals gap, driving the crossover from a 2D vibrational (i.e., interlayer decoupled) system toward an effectively 3D system (i.e., coupled across neighboring layers).

We note that the modes ω_+ and ω_- in this heterobilayer system are in analogy to the A_{1g} (in-phase) and B_{1u} (out-of-phase) oscillation modes usually defined in homobilayers [18]. In the case of naturally AB -stacked homobilayers, however, the B_{1u} mode is Raman-inactive forbidden by its symmetry [18]. In contrast, both ω_+ and ω_- are Raman active in our heterobilayers due to relaxation of the symmetry rule by the random stacking configurations in the WS_2/MoS_2 heterobilayers. However, it is interesting to note the opposite trends of intensity of the ω_+ and ω_- peaks as seen in Fig. 2(a): As pressure increases, the intensity of ω_+ is enhanced and that of ω_- is reduced. This can be attributed to a residual effect of the different degrees of Raman activity of the A_{1g} and B_{1u} modes in the homobilayers. We also note that a similar mode repulsion has been observed in bulk InSe crystals under hydrostatic pressures below $\sim 15 \text{ GPa}$ [26,27]. However, we also note the difference: In our Rapid Communication, we probe vibration in membranes of truly atomic thicknesses, and the repulsion in our Rapid Communication is between two identical modes, which is possible in our experiments because they are from MoS_2 and WS_2 , respectively, and are thus spectrally distinguishable.

In conclusion, using a diamond-anvil cell, the interlayer coupling between MoS_2 and WS_2 monolayers is mechanically modulated. As a result, the out-of-plane vibration of the system is strongly renormalized, resulting in two coherent vibration modes involving the sulfur atoms in the two monolayers to vibrate in and out of phase, respectively. The effect discovered here shows that the vibrational structure of layered materials can be artificially and reversibly modulated across the van der Waals gap, providing a means to probe dimensionality effects of 2D materials.

This work was supported by the National Science Foundation under Grant No. DMR-1306601. H.S. is grateful for the hospitality from Dr. J. Vasbinder at the Institute Para Limes in the early stage of this work. W.F. gratefully acknowledges Dr. J. Yan for help with the DAC setup and Professor F. Wang for useful discussions. The laser milling

was supported by COMPRES (Grant No. EAR 11-57758). K.D. acknowledges the Chinese Scholarship Council (CSC, Grant No. 201406210211) for financial support. J.W., J.W.A., and Y.C. acknowledge support from the Singapore-Berkeley Research Initiative for Sustainable Energy (SinBeRISE).

W.F. and X.Z. contributed equally to this work.

- [1] Q. H. Wang, K. Kalantar-Zadeh, A. Kis, J. N. Coleman, and M. S. Strano, Electronics and optoelectronics of two-dimensional transition metal dichalcogenides, *Nat. Nanotechnol.* **7**, 699 (2012).
- [2] A. K. Geim and I. V. Grigoriev, Van der Waals heterostructures, *Nature (London)* **499**, 419 (2013).
- [3] S. Tongay, H. Sahin, C. Ko, A. Luce, W. Fan, K. Liu, J. Zhou, Y.-S. Huang, C.-H. Ho, J. Yan, D. F. Ogletree, S. Aloni, J. Ji, S. Li, Jingbo Li, F. M. Peeters, and J. Wu, Monolayer behaviour in bulk ReS₂ due to electronic and vibrational decoupling, *Nat. Commun.* **5**, 3252 (2014).
- [4] K. F. Mak, C. Lee, J. Hone, J. Shan, and T. F. Heinz, Atomically Thin MoS₂: A New Direct-Gap Semiconductor, *Phys. Rev. Lett.* **105**, 136805 (2010).
- [5] K. F. Mak, K. He, C. Lee, G. H. Lee, J. Hone, T. F. Heinz, and J. Shan, Tightly bound trions in monolayer MoS₂, *Nature Mater.* **12**, 207 (2012).
- [6] A. Splendiani, L. Sun, Y. Zhang, T. Li, J. Kim, C. Y. Chim, G. Galli, and F. Wang, Emerging photoluminescence in monolayer MoS₂, *Nano Lett.* **10**, 1271 (2010).
- [7] S. Tongay, J. Zhou, C. Ataca, K. Lo, T. S. Matthews, J. Li, J. C. Grossman, and J. Wu, Thermally driven crossover from indirect toward direct bandgap in 2D semiconductors: MoS₂ versus MoSe₂, *Nano Lett.* **12**, 5576 (2012).
- [8] G. W. Mudd, S. A. Svatek, T. Ren, A. Patanè, O. Makarovskiy, L. Eaves, P. H. Beton, Z. D. Kovalyuk, G. V. Lashkarev, Z. R. Kudrynskiy, and A. I. Dmitriev, Tuning the bandgap of exfoliated InSe nanosheets by quantum confinement, *Adv. Mater.* **25**, 5714 (2013).
- [9] S. Lei, L. Ge, S. Najmaei, A. George, R. Kappera, J. Lou, M. Chhowalla, H. Yamaguchi, G. Gupta, R. Vajtai, A. D. Mohite, and P. M. Ajayan, Evolution of the electronic band structure and efficient photo-detection in atomic layers of InSe, *ACS Nano* **8**, 1263 (2014).
- [10] A. P. Nayak, T. Pandey, D. Voiry, Jin Liu, S. T. Moran, A. Sharma, C. Tan, C.-H. Chen, L.-J. Li, M. Chhowalla, J.-F. Lin, A. K. Singh, and D. Akinwande, Pressure-dependent optical and vibrational properties of monolayer molybdenum disulfide, *Nano Lett.* **15**, 346 (2015).
- [11] Z. H. Chi, X. M. Zhao, H. Zhang, A. F. Goncharov, S. S. Lobanov, T. Kagayama, M. Sakata, and X. J. Chen, Pressure-Induced Metallization of Molybdenum Disulfide, *Phys. Rev. Lett.* **113**, 036802 (2014).
- [12] A. P. Nayak, S. Bhattacharyya, J. Zhu, Jin Liu, X. Wu, T. Pandey, C. Jin, A. K. Singh, D. Akinwande, J.-F. Lin, Pressure-induced semiconducting to metallic transition in multilayered molybdenum disulphide, *Nat. Commun.* **5**, 3731 (2014).
- [13] Y.-H. Lee, X.-Q. Zhang, W. Zhang, M.-T. Chang, C.-T. Lin, K.-D. Chang, Y.-C. Yu, J. T.-W. Wang, C.-S. Chang, L.-J. Li, and T.-W. Lin, Synthesis of large-area MoS₂ atomic layers with chemical vapor deposition, *Adv. Mater.* **24**, 2320 (2012).
- [14] S. Tongay, W. Fan, J. Kang, J. Park, U. Koldemir, J. Suh, D. S. Narang, K. Liu, J. Ji, J. Li, R. Sinclair, and J. Wu, Tuning interlayer coupling in large-area heterostructures with CVD-grown MoS₂ and WS₂ monolayers, *Nano Lett.* **14**, 3185 (2014).
- [15] C. Lee, H. Yan, L. E. Brus, T. F. Heinz, J. Hone, and S. Ryu, Anomalous lattice vibrations of single- and few-layer MoS₂, *ACS Nano* **4**, 2695 (2010).
- [16] K. Liu, L. Zhang, T. Cao, C. Jin, D. Qiu, Q. Zhou, A. Zettl, P. Yang, S. G. Louie, and F. Wang, Evolution of interlayer coupling in twisted molybdenum disulfide bilayers, *Nat. Commun.* **5**, 4966 (2014).
- [17] P. Tonndorf, R. Schmidt, P. Böttger, X. Zhang, J. Börner, A. Liebig, M. Albrecht, C. Kloc, O. Gordan, D. R. T. Zahn, S. M. de Vasconcellos, and R. Bratschitsch, Photoluminescence emission and Raman response of monolayer MoS₂, MoSe₂, and WSe₂, *Opt. Express* **21**, 4908 (2013).
- [18] A. Molina-Sanchez and L. Wirtz, Phonons in single-layer and few-layer MoS₂ and WS₂, *Phys. Rev. B* **84**, 155413 (2011).
- [19] B. Delley, An all-electron numerical method for solving the local density functional for polyatomic molecules, *J. Chem. Phys.* **92**, 508 (1990).
- [20] B. Delley, From molecules to solids with the DMol³ approach, *J. Chem. Phys.* **113**, 7756 (2000).
- [21] S. Grimme, Semiempirical GGA-type density functional constructed with a long-range dispersion correction, *J. Comput. Chem.* **27**, 1787 (2006).
- [22] J. P. Perdew, K. Burke, and M. Ernzerhof, Generalized Gradient Approximation Made Simple, *Phys. Rev. Lett.* **77**, 3865 (1996).
- [23] P. Raybaud, G. Kresse, J. Hafner, and H. Toulhoat, Ab initio density functional studies of transition-metal sulphides: I. Crystal structure and cohesive properties, *J. Phys.: Condens. Matter* **9**, 11085 (1997).
- [24] Y. Ding and B. Xiao, Thermal expansion tensors, Grüneisen parameters and phonon velocities of bulk MT₂ (M = W and Mo; T = S and Se) from first principles, *RSC Adv.* **5**, 18391 (2015).
- [25] D. Fu, J. Zhou, S. Tongay, K. Liu, W. Fan, T.-J. King, and J. Wu, Mechanically modulated tunneling resistance in monolayer MoS₂, *Appl. Phys. Lett.* **103**, 183105 (2013).
- [26] I.-H. Choi and P. Y. Yu, Pressure dependence of phonons and excitons in InSe films prepared by metal-organic chemical vapor deposition, *Phys. Rev. B* **68**, 165339 (2003).
- [27] D. Errandonea, D. Martínez-García, A. Segura, J. Haines, E. Machado-Charry, E. Canadell, J. C. Chervin, and A. Chevy, High-pressure electronic structure and phase transitions in monoclinic InSe: X-ray diffraction, Raman spectroscopy, and density functional theory, *Phys. Rev. B* **77**, 045208 (2008).